A modified inertial Tseng's algorithm with adaptive parameters for solving monotone inclusion problems with efficient applications to image deblurring problems

Purit Thammasiri[1] , Rabian Wangkeeree[1,2] , Kasamsuk Ungchittrakool[1,2*]

[1]Department of Mathematics, Faculty of Science, Naresuan University, Phitsanulok 65000, Thailand
[2]Center of Excellence in Mathematics, Faculty of Science, Naresuan University, Phitsanulok 65000, Thailand
Email:purit.thammasiri@gmail.com[1], rabianw@nu.ac.th[2], kasamsuku@nu.ac.th[3]
*Corresponding Author

Received: 10.09.2024 Revised: 20.09.2024 Accepted: 22.09.2024

ABSTRACT
In this paper, we have found a method to make use of some adaptive step size parameters to increase the algorithm's efficiency and produce superior numerical results. We introduce and study a modified inertial Tseng's algorithm with adaptive terms for solving the sum of two monotone inclusion problems in order to result in effective applications to solve image deblur- ring problems in the framework of realHilbert spaces. We achieve weak convergence to a zero point of the sum of two monotone operators by restricting the scalar control conditions, utilizing certain monotone operator properties, and using the identity associated with the norm square. Furthermore, a novel suggested algorithm is applied to image deblurring problems as part of the applications of this recently obtained theoretical knowledge. To illustrate the strong points and benefits of this recently suggested algorithm, we express some advantages in numerical tests on the signal-to-noise ratio (ISNR) and structural similarity index measure (SSIM) comparing with some previous related methods.

Keywords: Tseng's algorithm, adaptive parameter, monotone operator, monotone inclusion problem, image deblurring problem

1. INTRODUCTION

Throughout this paper, $\mathbb{N}$, $\mathbb{R}$, $\mathbb{R}^m$, $\mathbb{R}^{k\times l}$, and I denote, respectively, the set of all natural numbers, the set of all real numbers, the m-dimensional Euclidean space ($m\in\mathbb{N}$), the set of all $k\times l$ real matrices ($k,l\in\mathbb{N}$), and the identity mapping.

The process of eliminating blurry artifacts from an image to enhance its quality is known as image deblurring. The mathematical purpose of image deblurring is to reconstruct a blurred image y to its original state x as closely as possible. It can express the relationship between $x\in\mathbb{R}^{l\times 1}$ and $y\in\mathbb{R}^{k\times 1}$ in the form of a mathematical model as follows:

$$y = Bx+\eta,$$

where the blur operator is $B\in\mathbb{R}^{k\times l}$, and the noise is $\eta\in\mathbb{R}^{n\times 1}$. To obtain the reconstructed image, one can solve the following least-squares problem:

$$\text{find } x\in\arg\min_{x\in\mathbb{R}^{l\times 1}}\left\{\frac{1}{2}\|Bx-y\|_2^2+\tau\|x\|_1\right\}, \tag{1.1}$$

where the usual norm, the regularization parameter, and the l_1 norm are denoted by $\|\cdot\|_2$, τ, and $\|\cdot\|_1$, respectively. Let $\phi:\mathbb{R}^{l\times 1}\to\mathbb{R}$ be defined via $\phi(x)=\frac{1}{2}\|Bx-y\|_2^2$ and let $\psi:\mathbb{R}^{l\times 1}\to\mathbb{R}$ be defined via $\psi(x)=\tau\|x\|_1$. By defining Q as the gradient of ϕ, that is,

$$Q := \nabla\phi = \nabla\left(\frac{1}{2}\|B(\cdot)-y\|_2^2\right) = B^T(B(\cdot)-y),$$

(B^T is the transpose of B) and R as the sub differential of ψ, that is,

$$R := \partial\psi(x) = \left\{z \in H \mid \psi(w) \geq \psi(x) + \langle z, w-x\rangle, \forall w \in H\right\},$$

the monotone inclusion problem, which corresponds to the image deblurring problem (1.1), can be expressed by the following problem:

$$\text{find } x \in \mathbb{R}^{l\times 1} \text{ such that } 0 \in (Q+R)x, \quad (1.2)$$

Many authors proposed several methods to demonstrate their algorithm performance of improvement in signal-to-noise ratio (ISNR) and the structural similarity index measure (SSIM). The goal was to obtain advantageous numerical results in various forms and/or that could be applied to image deblurring problems in order to obtain the good quality of the restored image, see, for instance [1-8].

Given a real Hilbert space H, its inner product $\langle\cdot,\cdot\rangle$, and its induced norm $\|\cdot\| = \sqrt{\langle\cdot,\cdot\rangle}$, we let $Q: H \to H$ as a single-valued operator and $R: H \to 2^H$ as a multi-valued operator. Then Q is said to be:

1. firmly nonexpansive if $\|Q\mu - Qv\|^2 \leq \langle Q\mu - Qv, \mu - v\rangle, \quad \forall \mu, v \in H$,
   a. or identically, if
   $\|Q\mu - Qv\|^2 \leq \|\mu - v\|^2 - \|(I-Q)\mu - (I-Q)v\|^2, \quad \forall \mu, v \in H$
2. Lipschitzor Lipschitz continuous if there exists a constant $L \geq 0$ such that $\|Q\mu - Qv\| \leq L\|\mu - v\|, \quad \forall \mu, v \in H$. Specifically, Q is called a nonexpansive operator in the case of $L = 1$.

The graph of R is represented by $G(R) := \left\{(\mu, v) \in H \times H \mid v \in R\mu\right\}$ and the set of all zero points of R is written by $zer(R) := R^{-1}(0) = \{z \in H \mid 0 \in Rz\}$. Next, R is said to be:

1. monotone if $\langle \mu - v, \tilde{\mu} - \tilde{v}\rangle \geq 0, \quad \forall(\mu, \tilde{\mu}), (v, \tilde{v}) \in G(R)$ (It can be reduced to $\langle \mu - v, R\mu - Rv\rangle \geq 0, \quad \forall \mu, v \in H$ if R is single-value.);
2. $\kappa-$cocoercive (or $\kappa-$inverse strongly monotone) if there is $\kappa > 0$ such that $\langle \mu - v, \tilde{\mu} - \tilde{v}\rangle \geq \kappa\|\tilde{\mu} - \tilde{v}\|^2, \quad \forall(\mu, \tilde{\mu}), (v, \tilde{v}) \in G(R)$ (It can be reduced to $\langle \mu - v, R\mu - Rv\rangle \geq \kappa\|R\mu - Rv\|^2, \quad \forall \mu, v \in H$ if R is single-value.);
3. maximally monotone if R is monotone and $G(R)$ is not properly contained in any graph of other multi-valued monotone operator, that is, if $\hat{R}: H \to 2^H$ is a multi-valued monotone operator such that $G(R) \subseteq G(\hat{R})$, then $G(R) = G(\hat{R})$.

Note that $J_r^R = (I + rR)^{-1}$ for some $r > 0$ represents the resolvent of the multi-valued operator $R: H \to 2^H$. It is widely known that $D(J_r^R) = H$ (where $D(J_r^R)$ is the domain of J_r^R) and $J_r^R: H \to H$ is a single-valued and firmly nonexpansive operator if R is maximally monotone and $r > 0$. For further information, see [9-13].

Assume we have a single-valued operator $Q: H \to H$ and a multi-valued operator $R: H \to 2^H$. Next, the following is the expression of the inclusion problemfor the sum of these two operators:

$$\text{find } z \in H \text{ such that } z \in zer(Q+R) (\equiv 0 \in (Q+R)z). \quad (1.3)$$

The mathematical problem (1.3) is of significant interest because it is the general form of (1.2) and it has implications for many real-world applications, such as image restoration, signal processing, computer vision, convex minimization, fixed point problems, variational inequality, and more; see, for example [1-3, 6, 7, 14-16]. Notice that the representation of the fixed-point problem for the operator $S: H \to H$ is as follows:

$$\text{find } p \in H \text{ such that } p \in Fix(S), \quad (1.4)$$

where $Fix(S) := \{x \in H \mid Sx = x\}$. Additionally, Lemma 2.2in the next section illustrates the strong connection between (1.3) and (1.4).

Several authors have been inspired to create and enhance several methods to solve the problem of (1.3) due to the interest in its broad variety of applications. One popular method is the well-known forward-backward splitting method (FBSM), which was introduced in the following manner by Passty[2] and Lions and Mercier [1]:

$$u_{n+1} = (I + \lambda_n R)^{-1}(I - \lambda_n Q)(u_n), \quad (1.5)$$

where $(I - \lambda_n Q)$ is the forward step and $(I + \lambda_n R)^{-1}$ is the backward step. The weak convergence of (1.5) to a solution of (1.3) was shown by them under some suitable assumptions of $\{\lambda_n\}$. On the other hand, the concept of inertial extrapolation term $\zeta_n(u_n - u_{n-1})$ was introduced by Polyak[5] in 1964 as a way to accelerate convergence. As may be seen, for instance, in [4, 6, 7, 17-26], authors have since given the inertial extrapolation approach a significant deal of attention and have explored and improved it widely.

An inertial proximal technique was presented in 2001 by Alvarez and Attouch[4] for estimating $z \in zer(R)$, where $R: H \to 2^H$ is a maximally monotone operator. The procedure works as follows:

$$u_{n+1} = (I + \lambda_n R)^{-1}(u_n + \zeta_n(u_n - u_{n-1})), \quad (1.6)$$

where $\lambda_n > 0$ and $\zeta_n \in [0,1)$ meet certain suitable assumptions. Under the following condition

$$\sum_{n=1}^{\infty} \zeta_n \|u_n - u_{n-1}\|^2 < +\infty, \quad (1.7)$$

they can show that (1.6) converges weakly to a point $z \in zer(R)$.

Using an inertial extrapolation term, Moudafi and Oliny[7] developed the following method in 2003 to solve (1.3):

$$\begin{cases} v_n = u_n + \zeta_n(u_n - u_{n-1}), \\ u_{n+1} = (I + \lambda_n R)^{-1}(v_n - \lambda_n Q u_n), \end{cases} \quad (1.8)$$

where Q and R are maximally monotone operators with Q is κ-cocoercive. The weak convergence of (1.8) is achieved under some useful conditions, such as $\lambda_n < 2\kappa$, (1.7), and further on. In addition, since Q maps the vector u_n, we can conclude that (1.8) is not organized in a forward-backward manner.

In 2015, Lorenz and Pock [6] presented a new method for solving (1.3) that combined the inertial technique and the forward-backward method. Their iterative process is established as follows:

$$(\textbf{LP2015}) \begin{cases} v_n = u_n + \zeta_n(u_n - u_{n-1}), \\ u_{n+1} = (I + \lambda_n R)^{-1}(I - \lambda_n Q)(v_n), \end{cases} \quad (1.9)$$

where $0 \le \zeta_n \le \zeta < 1$, $Q, R: H \to 2^H$ are maximally monotone with Q is single-valued and cocoercive. They verified the weak convergence of (1.9) to a solution of (1.3) under certain assumptions, such as $\lambda_n > 0$, (1.7), and so forth. In addition, they employed (1.9) to address image processing problems and produced outcomes that were numerically superior to those reported in earlier studies.

Alternatively, Tseng [3] introduced the creation of (1.5), which provides a step and enables them to achieve convergence under less constrained assumptions than the original method (1.5). The Tseng algorithm is expressed as follows:

$$\begin{cases} w_n = (I+\lambda_n R)^{-1}(I-\lambda_n Q)(v_n), \\ u_{n+1} = w_n - \lambda_n (Qw_n - Qv_n), \end{cases} \tag{1.10}$$

It is not difficult to notice that (1.10) can be written in the new form as:

$$u_{n+1} = \left((I-\lambda_n Q)(I+\lambda_n R)^{-1}(I-\lambda_n Q)+Q\right)\left(v_n\right). \tag{1.11}$$

(1.11) can be called as forward–backward–forward algorithm.
In 2018, Gibali and Thong [27] presented an interesting idea that uses a new step size parameter to make convergence more efficient. Their new step size parameter can be expressed as follows:

$$\sigma_{n+1} = \begin{cases} \min\left\{ \dfrac{\mu \|w_n - v_n\|}{\|Qw_n - Qv_n\|}, \sigma_n \right\}, & \text{if } Qw_n \neq Qv_n, \\ \sigma_n, & \text{otherwise} \end{cases}$$

where $\sigma_1 > 0$ and $\mu \in (0,1)$.

An inertial technique was applied to (1.10) by Padcharoen et al. [8] in 2021, and they produced superior numerical results than those of the earlier research. The definition of the iterative process they employed is:

$$(\textbf{PKKK2021}) \begin{cases} v_n = u_n + \zeta_n (u_n - u_{n-1}), \\ w_n = (I+\lambda_n R)^{-1}(I-\lambda_n Q)(v_n), \\ u_{n+1} = w_n - \lambda_n (Qw_n - Qv_n), \end{cases} \tag{1.12}$$

where $Q: H \to H$ is a Lipschitz monotone operator and $R: H \to 2^H$ is a maximally monotone operator. They can show that (1.12) converges weakly to an element in $zer(Q+R)$ with certain suitable assumptions on $\{\zeta_n\}$, $\{\lambda_n\}$, and any other related conditions.

Inspired by the above research works in this direction, our goal in this study is to introduce and investigate a modified inertial Tseng's algorithm with adaptive terms for solving the sum of two monotone inclusion problems in order to result in some effective applications to solve image deblurring problems in the framework of real Hilbert spaces. This method can be viewed as a more broadly applicable theoretical expansion. This novel technique can be used to solve deblurring problems for images within the Hilbert space framework. Additionally, we can produce numerical tests to demonstrate some of the new algorithm's advantageous behaviors and to contrast the numerical outcomes with those of the earlier, related algorithms in terms of improvement in the structural similarity index measure (SSIM) and signal-to-noise ratio (ISNR).

2. Preliminaries

This section collects a number of useful tools that are essential for proving the main theorem within the setting of real Hilbert spaces. These tools will be ” will be used throughout this$\to$used in the next section. The symbols “ ” and “ study to denote weak convergence and strong convergence, respectively.

Lemma2.1([11, 12]).Let H be a real Hilbert space. Then,

1. $\|x+y\|^2 = \|x\|^2 + 2\langle x,y\rangle + \|y\|^2 = \|x\|^2 - \|y\|^2 + 2\langle y, x+y\rangle, \quad \forall x,y \in H,$
2. $\|(1-r)x + ry\|^2 = (1-r)\|x\|^2 + r\|y\|^2 - r(1-r)\|x-y\|^2, \quad \forall r \in \square$ and $\forall x,y \in H$.

Lemma 2.2. Let $Q: H \to H$ be an operator on H and $R: H \to 2^H$ be a maximally monotone operator. Define $S_\lambda := (I+\lambda R)^{-1}(I-\lambda Q)$, $\lambda > 0$. Then we have

$$Fix(S_\lambda) = zer(Q+R), \quad \forall \lambda > 0.$$

Proof. Refer to [8, Lemma 1.], for instance.

Lemma 2.3.([28]).Let $Q: H \to H$ be a Lipschitz continuous and monotone operator and

$R: H \to 2^H$ be a maximally monotone operator. Then the operator $Q+R$ is a maximally monotone operator.

Lemma 2.4.([29]).Suppose that $\{\alpha_n\},\{\beta_n\},\{\epsilon_n\} \subseteq [0,+\infty)$ satisfy the following assumptions

$$\alpha_{n+1} \le \alpha_n + \beta_n(\alpha_n - \alpha_{n-1}) + \epsilon_n, \quad \forall n \ge 1, \sum_{n=1}^{\infty} \epsilon_n < +\infty,$$

where $0 \le \beta_n \le \beta < 1$ for all $n \in \mathbb{N}$. Then the following results hold true:

1. $\sum_{n=1}^{+\infty} [\alpha_n - \alpha_{n-1}]_+ < +\infty$, where $[t]_+ := \max\{t, 0\}$,
2. there is $\alpha^* \in [0,+\infty)$ such that $\lim_{n\to+\infty} \alpha_n = \alpha^*$.

The next lemma has significance for applying to the main theorem's proof. However, first let us focus on the following set, which is defined by $\omega_w(u_n) := \left\{ z \;\middle|\; \exists\{u_{n_k}\} \subseteq \{u_n\} \text{ such that } u_{n_k} \rightharpoonup z \right\}$. This is the set of all weak sequential cluster points of $\{u_n\}$.

Lemma2.5([30]).Suppose that $\emptyset \ne C \subseteq H$ and $\{u_n\} \subseteq H$ satisfy the following two properties:

1. for every $u \in C$, $\lim_{n\to\infty} \|u_n - u\|$ exists,
2. any weak sequential cluster point of $\{u_n\}$ is in C, that is, $\omega_w(u_n) \subseteq C$.

Then $\{u_n\}$ weakly converges to a point in C.

Lemma 2.6. Let $Q: H \to H$ be an operator and $R: H \to 2^H$ be a maximally monotone operator. Then, for any $v, w \in H$ together with $\rho > 0$, it will lead to the following equivalence:

$$w = (I+\rho R)^{-1}(I-\rho Q)v \quad \Leftrightarrow \quad \exists q \in Rw \text{ such that } q = \frac{1}{\rho}\left(v - w - \rho Qv\right).$$

Proof. Let us consider the following equivalence, which can be expressed as follows:

$$\begin{aligned} w = (I+\rho R)^{-1}(I-\rho Q)v \quad &\Leftrightarrow \quad v - \rho Qv \in w + \rho Rw \\ &\Leftrightarrow \frac{1}{\rho}\left(v - w - \rho Qv\right) \in Rw \\ &\Leftrightarrow \exists q \in Rw \text{ such that } q = \frac{1}{\rho}\left(v - w - \rho Qv\right). \end{aligned}$$

This completes the proof.

□

Lemma2.7. Let $Q: H \to H$ be a Lipschitz continuous and monotone operator and $R: H \to 2^H$ be a maximally monotone operator where H is a real Hilbert space. Then, for any $v, w \in H$ together with $\rho > 0$ such that $w = (I+\rho R)^{-1}(I-\rho Q)v$ and $z \in zer(Q+R)$, the following in equality holds:

$$\left\langle v - w - \lambda\left(Qv - Qw\right), w - z \right\rangle \ge 0.$$

Proof.Since $w = (I+\rho R)^{-1}(I-\rho Q)v$, so by Lemma 2.6, there exists $q \in Rw$ such that $q = \frac{1}{\rho}\left(v - w - \rho Qv\right)$. On the other hand, since $0 \in (Q+R)z$ and $Qw + q \in Qw + Rw = (Q+R)w$. Thus, by Lemma 2.3, we get that

$$\left\langle (Qw+q) - 0, w - z \right\rangle \ge 0. \tag{2.1}$$

Note that

$$Qw+q=Qw+\frac{1}{\rho}\big(v-w-\rho Qv\big)=\frac{1}{\rho}\big(v-w-\rho(Qv-Qw)\big). \quad (2.2)$$

It follows from (2.1) and (2.2) that

$$\frac{1}{\rho}\langle v-w-\rho(Qv-Qw),w-z\rangle\geq 0. \quad (2.3)$$

Now, by multiplying both sides of (2.3) by ρ, we obtain

$$\langle v-w-\rho(Qv-Qw),w-z\rangle\geq 0.$$

This completes the proof.

□

Convergence Analysis

Condition3.1. The solution set of the inclusion problem (1.3) is non empty, that is, $zer(Q+R)\neq\emptyset$.

Condition3.2. Theoperator $Q:H\to H$ are Lipschitz monotone operator with the Lipschitz constant L, and $R:H\to 2^H$ are maximally monotone operators.

Weak convergence

In this subsection, we present and study a modified inertial Tseng algorithm with adaptive parameters for finding a zero point of the sum of two monotone operators as follows:

Algorithm 1

Initialization: Given $\sigma_1\geq 0$, $\mu\in(0,1)$, $\{c_n\}\subseteq[0,1]$, $\{\lambda_n\}\subseteq[a,b]\subseteq[a,\sigma+b]\subseteq\left(0,\frac{1}{L}\right)$, where $\sigma=\lim_{n\to\infty}\sigma_n\left(\sigma_n\downarrow\sigma \text{ as } n\to\infty\right)$, see more details from Lemma 3.3 and $\{\zeta_n\}\subseteq[0,\zeta]\subseteq[0,1)$. Let $u_0,u_1\in H$ be arbitrary.

Iterative Steps: Given the current iterates $u_{n-1},u_n\in H$, calculate the next iterate as follows:

Compute

$$\begin{cases} v_n=u_n+\zeta_n(u_n-u_{n-1}),\\ w_n=(I+(\sigma_n+c_n\lambda_n)R)^{-1}(I-(\sigma_n+c_n\lambda_n)Q)v_n,\\ u_{n+1}=w_n-(\sigma_n+c_n\lambda_n)(Qw_n-Qv_n),\end{cases}$$

Update

$$\sigma_{n+1}=\begin{cases}\min\left\{\frac{\mu\|w_n-v_n\|}{\|Qw_n-Qv_n\|},\sigma_n\right\}, & \text{if } Qw_n\neq Qv_n,\\ \sigma_n & \text{, otherwise.}\end{cases}$$

Set $n:=n+1$.

Lemma3.3 The generated sequence $\{\sigma_n\}$ is monotonically nonincreasing and bounded from below by $\min\left\{\frac{\mu}{L},\sigma_1\right\}$.

Proof.It is clear from the definition of $\{\sigma_n\}$ that it is monotonically nonincreasing, that is, $\sigma_{n+1}\leq\sigma_n$ for all $n\in\mathbb{N}$. Since Q is a Lipschitz operator with Lipschitz's constant L, for $Qw_n\neq Qv_n$, we have:

$$\frac{\mu\|w_n-v_n\|}{\|Qw_n-Qv_n\|}\geq\frac{\mu}{L}$$

Therefore, it is not hard to see that $\min\left\{\frac{\mu}{L},\sigma_1\right\}$ is the lower bound of $\{\sigma_n\}$. □

Remark3.4 By Lemma 3.3, the update in **Algorithm 1** is well defined and
$\sigma_{n+1}\|Qw_n-Qv_n\|\le\mu\|w_n-v_n\|$.

Lemma3.5 Assume that **Condition 1**and **Condition 2** hold and let $\{u_n\}$ be the sequence generated by **Algorithm 1**. Then, for any $z\in zer(Q+R)$, there exists $n_0\in\mathbb{N}$ such that

$1-(\sigma_n+b)^2L^2>0,\quad \forall n\ge n_0$

and the following inequality holds:

$$\|u_{n+1}-z\|^2\le\|v_n-z\|^2-\left(1-(\sigma_{n_0}+b)^2L^2\right)\|w_n-v_n\|^2,\quad \forall n\ge n_0. \tag{3.1}$$

Proof.For any $z\in zer(Q+R)$, we can apply Lemma 2.1(1) and Lemma (2.7) that will allow us to obtain the following inequality

$$\begin{aligned}
&\|u_{n+1}-z\|^2\\
&=\|w_n-z-(\sigma_n+c_n\lambda_n)(Qw_n-Qv_n)\|^2\\
&=\|w_n-z\|^2-2(\sigma_n+c_n\lambda_n)\langle w_n-z,Qw_n-Qv_n\rangle+(\sigma_n+c_n\lambda_n)^2\|Qw_n-Qv_n\|^2\\
&\le\|(v_n-z)+(w_n-v_n)\|^2+2(\sigma_n+c_n\lambda_n)\langle Qv_n-Qw_n,w_n-z\rangle+(\sigma_n+c_n\lambda_n)^2L^2\|w_n-v_n\|^2\\
&=\|v_n-z\|^2-\|w_n-v_n\|^2+2\langle w_n-v_n,w_n-z\rangle+2(\sigma_n+c_n\lambda_n)\langle Qv_n-Qw_n,w_n-z\rangle\\
&\quad+(\sigma_n+c_n\lambda_n)^2L^2\|w_n-v_n\|^2\\
&\le\|v_n-z\|^2-\|w_n-v_n\|^2-2\langle v_n-w_n-(\sigma_n+c_n\lambda_n)(Qv_n-Qw_n),w_n-z\rangle\\
&\quad+(\sigma_n+b)^2L^2\|w_n-v_n\|^2\\
&\le\|v_n-z\|^2-\left(1-(\sigma_n+b)^2L^2\right)\|w_n-v_n\|^2.
\end{aligned}$$

(3.2)

Since $\sigma_n\downarrow\sigma$ as $n\to\infty$ and $\sigma+b<\frac{1}{L}$, so $\exists n_0\in\mathbb{N}$ such that $1-(\sigma_n+b)^2L^2>0,\quad\forall n\ge n_0$ and (3.2) holds for all $n\ge n_0$. In particular, since $\{\sigma_n\}$ is monotonically decreasing, so $\sigma_n\le\sigma_{n_0},\quad\forall n\ge n_0$ and then

$$\begin{aligned}
\|u_{n+1}-z\|^2&\le\|v_n-z\|^2-\left(1-(\sigma_n+b)^2L^2\right)\|w_n-v_n\|^2\\
&\le\|v_n-z\|^2-\left(1-(\sigma_{n_0}+b)^2L^2\right)\|w_n-v_n\|^2,\quad\forall n\ge n_0.
\end{aligned}$$

This completes the proof.
□

Lemma3.6 Suppose that **Condition 1** and **Condition 2** hold. Let $\{w_n\},\{v_n\}$ be the sequences generated by **Algorithm 1**. If $\lim_{n\to\infty}\|v_n-w_n\|=0$ and $\{w_{n_k}\}$ converge weakly to $z\in H$, then $z\in zer(Q+R)$.

Proof.Suppose that $\lim_{n\to\infty}\|v_n-w_n\|=0$. Then, it follows from the definition of **Algorithm 1** that

$$w_{n_k}=(I+(\sigma_{n_k}+c_{n_k}\lambda_{n_k})R)^{-1}(I-(\sigma_{n_k}+c_{n_k}\lambda_{n_k})Q)v_{n_k},$$

andso it follows from the implications of Lemma 2.6and cause the following

$$\frac{1}{(\sigma_{n_k}+c_{n_k}\lambda_{n_k})}\left(v_{n_k}-w_{n_k}-(\sigma_{n_k}+c_{n_k}\lambda_{n_k})Qv_{n_k}\right)\in Rw_{n_k}.$$

Let $(x,y)\in G(Q+R)$. Then, $y\in(Q+R)x$, that is, $y-Qx\in Rx$. And by monotonicity of R, it allows that

$$\left\langle x - w_{n_k}, y - Qx - \frac{1}{(\sigma_{n_k} + c_{n_k}\lambda_{n_k})}\left(v_{n_k} - w_{n_k} - (\sigma_{n_k} + c_{n_k}\lambda_{n_k})Qv_{n_k}\right)\right\rangle \geq 0.$$

(3.3)

We can write (3.3) to be the new form as follows

$$\begin{aligned}
\left\langle x - w_{n_k}, y\right\rangle &\geq \left\langle x - w_{n_k}, Qx + \frac{1}{(\sigma_{n_k} + c_{n_k}\lambda_{n_k})}\left(v_{n_k} - w_{n_k} - (\sigma_{n_k} + c_{n_k}\lambda_{n_k})Qv_{n_k}\right)\right\rangle \\
&= \left\langle x - w_{n_k}, Qx - Qv_{n_k}\right\rangle + \left\langle x - w_{n_k}, \frac{1}{(\sigma_{n_k} + c_{n_k}\lambda_{n_k})}\left(v_{n_k} - w_{n_k}\right)\right\rangle \\
&= \left\langle x - w_{n_k}, Qx - Qw_{n_k}\right\rangle + \left\langle x - w_{n_k}, Qw_{n_k} - Qv_{n_k}\right\rangle \\
&\quad + \left\langle x - w_{n_k}, \frac{1}{(\sigma_{n_k} + c_{n_k}\lambda_{n_k})}\left(v_{n_k} - w_{n_k}\right)\right\rangle \\
&\geq \left\langle x - w_{n_k}, Qw_{n_k} - Qv_{n_k}\right\rangle + \left\langle x - w_{n_k}, \frac{1}{(\sigma_{n_k} + c_{n_k}\lambda_{n_k})}\left(v_{n_k} - w_{n_k}\right)\right\rangle.
\end{aligned}$$

Since $\lim_{n\to\infty}\|v_n - w_n\| = 0$ and Q is a Lipschitz operator, we obtain $\lim_{k\to\infty}\left\|Qw_{n_k} - Qv_{n_k}\right\| = 0$ and since $(\sigma_n + c_n\lambda_n)$ is bounded, we have

$$\left\langle x - z, y - 0\right\rangle = \left\langle x - z, y\right\rangle = \lim_{n\to\infty}\left\langle x - w_{n_k}, y\right\rangle \geq 0.$$

By the virtue of Lemma 2.3, we can conclude that $0 \in (Q+R)z$, that is, $z \in zer(Q+R)$. □

Theorem3.7 Suppose that **Condition1** and **Condition2** hold. Let n_0 be a natural number that comes from Lemma3.5 and let $\{\zeta_n\}$ be a nondecreasing sequence such that

$$0 \leq \zeta_n \leq \zeta < \frac{\sqrt{1+8\varepsilon} - 1 - 2\varepsilon}{2(1-\varepsilon)}, \tag{3.4}$$

where $\varepsilon = \dfrac{1-(\sigma_{n_0}+b)L}{1+(\sigma_{n_0}+b)L}$. Then, the sequence $\{u_n\}$ generated by **Algorithm 1** converges weakly to $\tilde{z} \in zer(Q+R)$.

Proof.Let $z \in zer(R+Q)$ and for any $n \geq n_0$. Then, let us consider the inequality below

$$\|u_{n+1} - w_n\| = \|w_n - (\sigma_n + c_n\lambda_n)(Qw_n - Qv_n) - w_n\| \leq (\sigma_n + c_n\lambda_n)L\|w_n - v_n\|. \tag{3.5}$$

By connecting (3.5) to the following inequality, we obtain

$$\begin{aligned}
\|u_{n+1} - v_n\| &\leq \|u_{n+1} - w_n\| + \|w_n - v_n\| \leq \left(1 + (\sigma_n + c_n\lambda_n)L\right)\|w_n - v_n\| \\
&\leq \left(1 + (\sigma_{n_0} + b)L\right)\|w_n - v_n\|,
\end{aligned}$$

which implies

$$-\|w_n - v_n\|^2 \leq -\frac{1}{\left(1 + (\sigma_{n_0} + b)L\right)^2}\|u_{n+1} - v_n\|^2. \tag{3.6}$$

Multiplying both sides of (3.6) by $1 - (\sigma_{n_0} + b)^2 L^2$ and then connecting with (3.1) it yields that

$$\|u_{n+1}-z\|^2 \le \|v_n-z\|^2-\left(1-(\sigma_{n_0}+b)^2L^2\right)\|w_n-v_n\|^2$$
$$\le \|v_n-z\|^2-\frac{\left(1-(\sigma_{n_0}+b)^2L^2\right)}{\left(1+(\sigma_{n_0}+b)L\right)^2}\|u_{n+1}-v_n\|^2$$
$$=\|v_n-z\|^2-\frac{\left(1-(\sigma_{n_0}+b)L\right)}{\left(1+(\sigma_{n_0}+b)L\right)}\|u_{n+1}-v_n\|^2$$
$$=\|v_n-z\|^2-\varepsilon\|u_{n+1}-v_n\|^2, \qquad (3.7)$$

where $\varepsilon:=\frac{1-(\sigma_{n_0}+b)L}{1+(\sigma_{n_0}+b)L}$. By the definition of v_n, and using Lemma 2.1(2.), we obtain the following equation

$$\|v_n-z\|^2=\|(1+\zeta_n)(u_n-z)-\zeta_n(u_{n-1}-z)\|^2$$
$$=\left(1+\zeta_n\right)\|u_n-z\|^2-\zeta_n\|u_{n-1}-z\|^2+\zeta_n\left(1+\zeta_n\right)\|u_n-u_{n-1}\|^2. \quad (3.8)$$

It follows from (3.7) and (3.8) that

$$\|u_{n+1}-z\|^2 \le \|v_n-z\|^2-\varepsilon\|u_{n+1}-v_n\|^2$$
$$=\left(1+\zeta_n\right)\|u_n-z\|^2-\zeta_n\|u_{n-1}-z\|^2+\zeta_n\left(1+\zeta_n\right)\|u_n-u_{n-1}\|^2-\varepsilon\|u_{n+1}-v_n\|^2$$
$$\le\left(1+\zeta_n\right)\|u_n-z\|^2-\zeta_n\|u_{n-1}-z\|^2+\zeta_n\left(1+\zeta_n\right)\|u_n-u_{n-1}\|^2. \qquad (3.9)$$

On the other hand, by employing Lemma 2.1(1.), Cauchy–Schwarz inequality, and AM-GM inequality, we achieve the following result

$$\|u_{n+1}-v_n\|^2=\|u_{n+1}-u_n-\zeta_n(u_n-u_{n-1})\|^2$$
$$=\|u_{n+1}-u_n\|^2+\zeta_n^2\|u_n-u_{n-1}\|^2-2\zeta_n\left\langle u_{n+1}-u_n,u_n-u_{n-1}\right\rangle$$
$$\ge\|u_{n+1}-u_n\|^2+\zeta_n^2\|u_n-u_{n-1}\|^2-2\zeta_n\|u_{n+1}-u_n\|\|u_n-u_{n-1}\|$$
$$\ge(1-\zeta_n)\|u_{n+1}-u_n\|^2+\left(\zeta_n^2-\zeta_n\right)\|u_n-u_{n-1}\|^2. \qquad (3.10)$$

Combining (3.8), (3.9) and (3.10) we obtain

$$\|u_{n+1}-z\|^2 \le \|v_n-z\|^2-\varepsilon\|u_{n+1}-v_n\|^2$$
$$\le(1+\zeta_n)\|u_n-z\|^2-\zeta_n\|u_{n-1}-z\|^2+\zeta_n(1+\zeta_n)\|u_n-u_{n-1}\|^2$$
$$-\varepsilon(1-\zeta_n)\|u_{n+1}-u_n\|^2-\varepsilon(\zeta_n^2-\zeta_n)\|u_n-u_{n-1}\|^2$$
$$=(1+\zeta_n)\|u_n-z\|^2-\zeta_n\|u_{n-1}-z\|^2-\varepsilon(1-\zeta_n)\|u_{n+1}-u_n\|^2$$
$$+\left(\zeta_n(1+\zeta_n)-\varepsilon(\zeta_n^2-\zeta_n)\right)\|u_n-u_{n-1}\|^2$$
$$=(1+\zeta_n)\|u_n-z\|^2-\zeta_n\|u_{n-1}-z\|^2$$
$$-\gamma_n\|u_{n+1}-u_n\|^2+\mu_n\|u_n-u_{n-1}\|^2, \qquad (3.11)$$

where $\gamma_n:=\varepsilon(1-\zeta_n)$ and $\mu_n:=\zeta_n(1+\zeta_n)-\varepsilon(\zeta_n^2-\zeta_n)\ge 0$. Then we set

$$\Upsilon_n:=\|u_n-z\|^2-\zeta_n\|u_{n-1}-z\|^2+\mu_n\|u_n-u_{n-1}\|^2.$$

Changing the writing style of (3.11) allows us to get that

$$\|u_{n+1}-z\|^2-\zeta_n\|u_n-z\|^2\le\|u_n-z\|^2-\zeta_n\|u_{n-1}-z\|^2-\gamma_n\|u_{n+1}-u_n\|^2+\mu_n\|u_n-u_{n-1}\|^2. \quad (3.12)$$

By adding $\mu_{n+1}\|u_{n+1}-u_n\|^2$ on both sides of (3.12), we have

$$\|u_{n+1}-z\|^2-\zeta_n\|u_n-z\|^2+\mu_{n+1}\|u_{n+1}-u_n\|^2$$
$$\le \|u_n-z\|^2-\zeta_n\|u_{n-1}-z\|^2+\mu_n\|u_n-u_{n-1}\|^2-\gamma_n\|u_{n+1}-u_n\|^2+\mu_{n+1}\|u_{n+1}-u_n\|^2.$$

Since $\{\zeta_n\}$ is nondecreasing, we get

$$\overbrace{\|u_{n+1}-z\|^2-\zeta_{n+1}\|u_n-z^*\|^2+\mu_{n+1}\|u_{n+1}-u_n\|^2}^{\Upsilon_{n+1}}$$
$$\le \overbrace{\|u_n-u^*\|^2-\zeta_n\|u_{n-1}-z\|^2+\mu_n\|u_n-u_{n-1}\|^2}^{\Upsilon_n}-(\gamma_n-\mu_{n+1})\|u_{n+1}-u_n\|^2,$$

which yields

$$\Upsilon_{n+1}-\Upsilon_n\le-(\gamma_n-\mu_{n+1})\|u_{n+1}-u_n\|^2. \tag{3.13}$$

It follows from $0\le\zeta_n\le\zeta_{n+1}\le\zeta$ that

$$\begin{aligned}\gamma_n-\mu_{n+1}&=\varepsilon(1-\zeta_n)-\zeta_{n+1}(1+\zeta_{n+1})+\varepsilon(\zeta_{n+1}^2-\zeta_{n+1})\\&=\varepsilon-\varepsilon\zeta_n-\zeta_{n+1}-\zeta_{n+1}^2+\varepsilon\zeta_{n+1}^2-\varepsilon\zeta_{n+1}\\&\ge\varepsilon-\varepsilon\zeta-\zeta-(1-\varepsilon)\zeta_{n+1}^2-\varepsilon\zeta\\&\ge\varepsilon-\varepsilon\zeta-\zeta-(1-\varepsilon)\zeta^2-\varepsilon\zeta\end{aligned}$$
$$=-(1-\varepsilon)\zeta^2-(1+2\varepsilon)\zeta+\varepsilon. \tag{3.14}$$

By merging (3.13) and (3.14), we obtain

$$\Upsilon_{n+1}-\Upsilon_n\le-\delta\|u_{n+1}-u_n\|^2, \tag{3.15}$$

where $\delta:=-(1-\varepsilon)\zeta^2-(1+2\varepsilon)\zeta+\varepsilon.$ By using condition (3.4) and solving the quadratic inequality it is not difficult to show that $\delta>0.$ Therefore

$$\Upsilon_{n+1}-\Upsilon_n\le 0.$$

Thusthe sequence $\{\Upsilon_n\}$ is nonincreasing. It can be observed that

$$\begin{aligned}\Upsilon_n&=\|u_n-z\|^2-\zeta_n\|u_{n-1}-u^*\|^2+\mu_n\|u_n-u_{n-1}\|^2\\&\ge\|u_n-z\|^2-\zeta_n\|u_{n-1}-z\|^2.\end{aligned}$$

This implies that

$$\begin{aligned}\|u_n-z\|^2&\le\zeta_n\|u_{n-1}-z\|^2+\Upsilon_n\\&\le\zeta\|u_{n-1}-z\|^2+\Upsilon_{n_0}\\&\le\ldots\le\zeta^{n-n_0}\|u_{n_0}-z\|^2+\Upsilon_{n_0}(\zeta^{n-n_0-1}+\ldots+1)\end{aligned}$$
$$\le\zeta^{n-n_0}\|u_{n_0}-z\|^2+\frac{\Upsilon_{n_0}}{1-\zeta}. \tag{3.16}$$

We also have

$$\Upsilon_{n+1}=\|u_{n+1}-z\|^2-\zeta_{n+1}\|u_n-z\|^2+\mu_{n+1}\|u_{n+1}-u_n\|^2$$
$$\ge-\zeta_{n+1}\|u_n-z\|^2. \tag{3.17}$$

From (3.16) and (3.17), we obtain

$$-\Upsilon_{n+1}\le\zeta_{n+1}\|u_n-z\|^2\le\zeta\|u_n-z\|^2\le\zeta^{n-n_0+1}\|u_{n_0}-z\|^2+\frac{\zeta\Upsilon_{n_0}}{1-\zeta}. \tag{3.18}$$

By using (3.15) and (3.18), along with some simple calculations, we get that

$$\begin{aligned}\delta\sum_{n=0}^{k}\|u_{n+1}-u_n\|^2 &= \delta\sum_{n=0}^{n_0-1}\|u_{n+1}-u_n\|^2+\delta\sum_{n=n_0}^{k}\|u_{n+1}-u_n\|^2\\ &\le M+\sum_{n=n_0}^{k}\left(\Upsilon_n-\Upsilon_{n+1}\right)=M+\Upsilon_{n_0}-\Upsilon_{k+1}\\ &\le M+\Upsilon_{n_0}+\zeta^{k-n_0+1}\|u_{n_0}-z\|^2+\frac{\zeta\Upsilon_{n_0}}{1-\zeta}\\ &\le M+\zeta\|u_{n_0}-z\|^2+\frac{\Upsilon_{n_0}}{1-\zeta},\end{aligned}$$

where $M:=\delta\sum_{n=0}^{n_0-1}\|u_{n+1}-u_n\|^2$. This implies $\sum_{n=0}^{\infty}\|u_{n+1}-u_n\|^2<+\infty$ and therefore

$$\lim_{n\to\infty}\|u_{n+1}-u_n\|=0. \tag{3.19}$$

On the otherhand we have

$$\|u_{n+1}-v_n\|^2=\|u_{n+1}-u_n\|^2+\zeta_n^2\|u_n-u_{n-1}\|^2-2\zeta_n\langle u_{n+1}-u_n,u_n-u_{n-1}\rangle,$$

and then get $\|u_{n+1}-v_n\|\to 0$ as $n\to\infty$. By (3.19) and Lemma 2.4, we have

$$\lim_{n\to\infty}\|u_n-z\|^2=l, \tag{3.20}$$

and by (3.8), we obtain

$$\|v_n-z\|^2=\|u_n-z\|^2+\zeta_n\left(\|u_n-z\|^2-\|u_{n-1}-z\|^2\right)+\zeta_n\left(1+\zeta_n\right)\|u_n-u_{n-1}\|^2. \tag{3.21}$$

Letting $n\to\infty$ in (3.21) and then (3.19) and (3.20) ensure that

$$\lim_{n\to\infty}\|v_n-z\|^2=l. \tag{3.22}$$

Moreover, it can be observed that $0\le\|u_n-v_n\|\le\|u_n-u_{n+1}\|+\|u_{n+1}-v_n\|$ for all $n\in\mathbb{N}$ and by letting $n\to\infty$, it will lead to

$$\lim_{n\to\infty}\|u_n-v_n\|=0. \tag{3.23}$$

On the other hand, as a consequence of (3.1) we obtain that

$$\left(1-(\sigma_{n_0}+b)^2L^2\right)\|w_n-v_n\|^2\le\|v_n-z\|^2-\|u_{n+1}-z\|^2. \tag{3.24}$$

Letting $n\to\infty$ in (3.24) and then (3.20) and (3.22) guarantee that

$$\lim_{n\to\infty}\|w_n-v_n\|=0. \tag{3.25}$$

Finally, we will prove that $u_n\rightharpoonup\tilde{z}$ for some $\tilde{z}\in zer(Q+R).$ Notice that the following statement "1) For every $z\in zer(Q+R),$ $\lim_{n\to\infty}\|u_n-z\|^2$ exists" is true via (3.20). Next, we let $z\in\omega_w(u_n)$ then there exists $\{u_{n_k}\}\subseteq\{u_n\}$ such that $u_{n_k}\rightharpoonup z$. Then, it is not hard to verify by using (3.23) that $v_{n_k}\rightharpoonup z$. Then, by applying (3.25) and Lemma 3.6, we can conclude that $z\in zer(Q+R)$. This means that "2) $\omega_w(u_n)\subseteq zer(Q+R)$". Therefore, by 1), 2) and Lemma 2.5 we conclude that $u_n\rightharpoonup\tilde{z}$ for some $\tilde{z}\in zer(Q+R).$ This completes the proof. □

Corollary 3.8 ([8, Theorem 1]). Let $Q:H\to H$ be a Lipschitz monotone operator, $R:H\to 2^H$ be a maximally monotone operator and $zer(Q+R)\neq\emptyset.$ Suppose that $\{\lambda_n\}\subseteq[a,b]\subseteq\left(0,\frac{1}{L}\right)$, $\{\zeta_n\}\subseteq[0,\zeta]\subseteq[0,1)$ is nondecreasing such that $0\le\zeta_n\le\zeta<\frac{\sqrt{1+8\varepsilon}-1-2\varepsilon}{2(1-\varepsilon)}$, where $\varepsilon=\frac{1-bL}{1+bL}$. Let $u_0,u_1\in H$ and the sequence $\{u_n\}$ be defined by

$$\begin{cases} v_n = u_n + \zeta_n (u_n - u_{n-1}), \\ w_n = (I + \lambda_n R)^{-1}(I - \lambda_n Q) v_n, \\ u_{n+1} = w_n - \lambda_n (Q w_n - Q v_n). \end{cases}$$

Then the sequence $\{u_n\}$ converges weakly to an element of $zer(Q+R)$.

Proof.In **Algorithm 1**, if we set $\sigma_1 = 0$ and set $c_n = 1$ for all $n \in \mathbb{N}$, then $\sigma_n = 0$ for all $n \in \mathbb{N}$. Therefore, Theorem 3.7can be reduced to Corollary 3.8as required. □

Applications to image deblurring problems and their numerical experiments

In this part, our goal is to recover an image using the suggested algorithm, tackling tasks such as image deblurring and denoising through a degradation model that effectively captures real-world difficulties in image restoration. We set the following: $Q = \nabla \phi(\cdot)$, and $R = \partial \psi(\cdot)$. Here, $\phi(x) = \frac{1}{2}\|Bx - y\|_2^2$, $\psi(x) = \tau \|x\|_1$, and $\tau = 0.001$. Given this setup, it follows that $\nabla \phi(x) = B^T(Bx - y)$, where the transpose of B is denoted as B^T. We initiated the problem-solving process by selecting images and applying various blurring techniques to them. We solve (1.1) by applying **Algorithm 1**, given the following condition: $\zeta_n = 0.9$, $\lambda_n = 0.5 - \frac{150n}{1000n+100}$, $c_n = 0.9$ and $\sigma_1 = 1$.We compare our proposed algorithm with the algorithm (LP2015) presented in [6], and the algorithm (PKKK2021) introduced by Padcharoen et al. [8].For the LP2015, We select parameter values as follows: $\zeta_n = 0.9$, and $\lambda_n = 0.5 - \frac{150n}{1000n+100}$. Concerning the PKKK2021, we select the following parameter values: $\zeta_n = 0.9$ and $\lambda_n = 0.5 - \frac{150n}{1000n+100}$. To evaluate the quality of the reconstructed image, we measure it by the structural similarity index measure (**SSIM**) [31] and the improvement in signal-to-noise ratio (**ISNR**) for images, which is defined as follows:

$$\mathbf{ISNR}(n) = 10 \log_{10} \frac{\|x - y\|_2^2}{\|x - x_n\|_2^2},$$

where x, y and x_n represent the original image, degraded image and the restored image at iteration n, respectively. The numerical results corresponding to the selections mentioned above are displayed in the following figures.

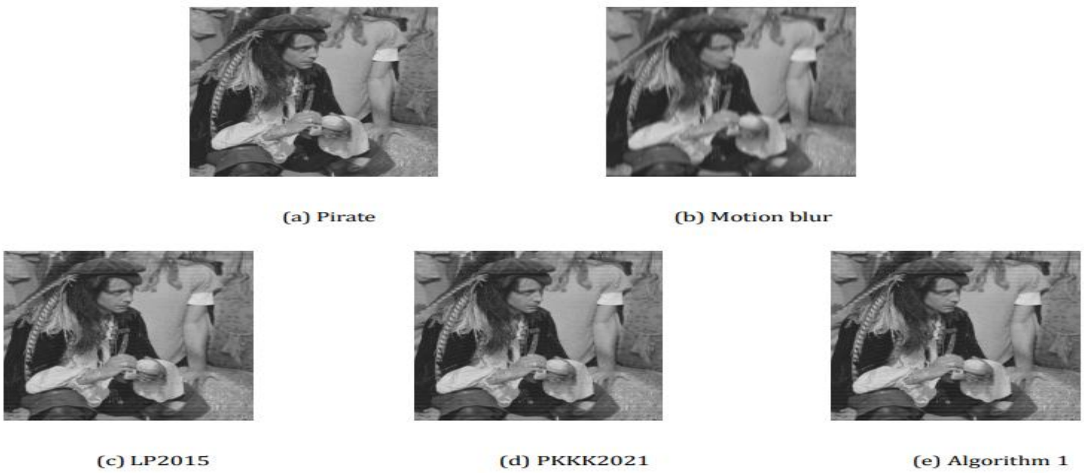

Figure 1: (a) shows the original 'Pirate' image, while (b) displays the images degraded by motion blur. The reconstructed images are depicted in (c), (d), and (e), corresponding to the results obtained using LP2015 [6], PKKK2021 [8], and Algorithm 1, respectively.

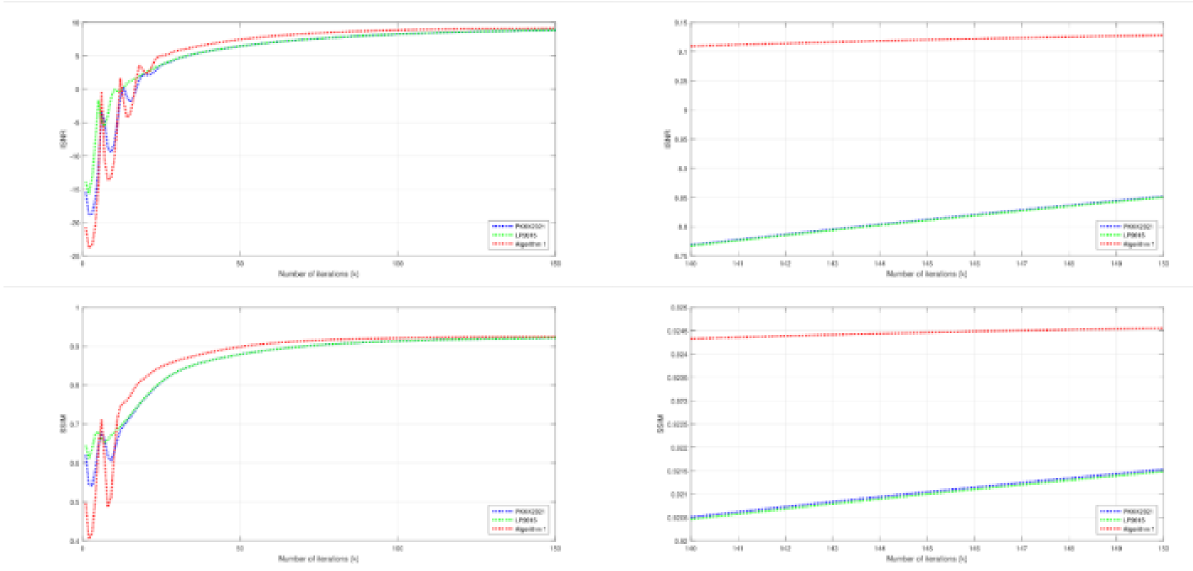

Figure 2: The figures illustrate the improvement in signal-to-noise ratio (ISNR) and structural similarity index measure (SSIM) performance for the three algorithms shown in Figure 1.

(a) Cameraman

(b) Average blur

(c) LP2015

(d) PKKK2021

(e) Algorithm 1

Figure 3: (a) shows the original 'Cameraman' image, while (b) displays the images degraded by average blur. The reconstructed images are depicted in (c), (d), and (e), corresponding to the results obtained using LP2015 [6], PKKK2021 [8], and Algorithm 1, respectively.

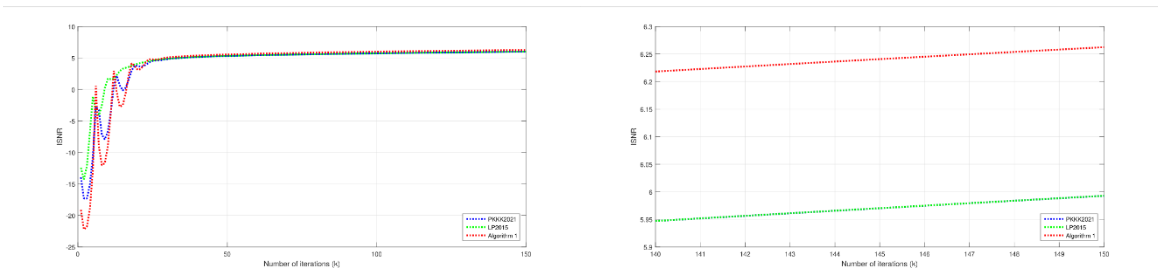

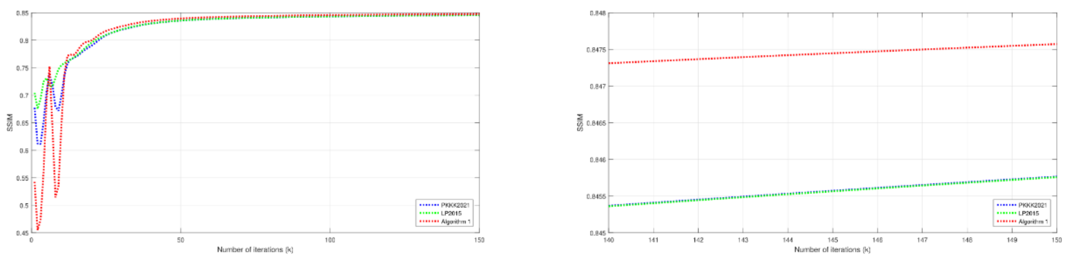

Figure 4: The figures illustrate the improvement in signal-to-noise ratio (ISNR) and structural similarity index measure (SSIM) performance for the three algorithms shown in Figure 3.

Table 1: The improvement in signal-to-noise ratio (ISNR) and structural similarity index measure (SSIM) are evaluated for"Pirate"images to assess their performance.

(n)		**ISNR**			**SSIM**	
	Algorithm 1	**PKKK2021**	**LP2015**	**Algorithm 1**	**PKKK2021**	**LP2015**
1	-20.7242	-15.4578	-13.8862	0.4970	0.6198	0.6453
10	-10.6439	-8.1584	-0.07185	0.6229	0.6275	0.6784
50	7.4501	6.4280	6.4293	0.8985	0.8789	0.8789
100	8.8444	8.2244	8.2234	0.9211	0.9131	0.9131
150	9.1277	8.8521	8.8506	0.9245	0.9215	0.9214

Table 2: The improvement in signal-to-noise ratio (ISNR) and structural similarity index measure (SSIM) are evaluated for"Cameraman"images to assess their performance.

(n)		**ISNR**			**SSIM**	
	Algorithm1	**PKKK2021**	**LP2015**	**Algorithm 1**	**PKKK2021**	**LP2015**
1	-19.1237	-13.9653	-12.4295	0.5424	0.6770	0.7041
10	-9.0430	-6.6542	1.7200	0.6471	0.7002	0.7547
50	5.5467	5.3170	5.3190	0.8394	0.8356	0.8357
100	5.9991	5.7303	5.7307	0.8456	0.8431	0.8431
150	6.2623	5.9927	5.9927	0.8475	0.8457	0.8457

The experimental results confirm that our algorithm has outperformedother methods, show-casing exceptional performance in image deblurring.

CONCLUSION

We created and investigated a modified inertial Tseng's algorithm with adaptive parameters for solving monotone inclusion problems with efficient applications to image deblurring problems, as appeared in Algorithm 1. We succeed in proving the weak convergence of Algorithm 1 by imposing some favorable conditions on the scalar terms and adaptive step size parameters, as well as the favorable property of monotone operators, as shown in Theorem 3.7. Furthermore, Algorithm 1 was utilized to address the image deblurring problem (1.1). Additionally, we conducted numerical experiments to evaluate the performance and demonstrated the bene- fits of Algorithm 1, specifically the enhancement in signal-to-noise ratio (ISNR) and structural similarity index measure (SSIM) measurements in contrast to certain other related algorithms that have been published previously. The higher performance of our method in the numerical tests reported in Section 4 clearly indicates that it has substantial advantages over some prior algorithms.

Acknowledgements

The authors would like to thank the editors and anonymous referees for their insightful feedback and recommendations that have improved the paper's quality and presentation. Furthermore, this work was supported by Naresuan University (NU), and National Science, Research and Innovation Fund (NSRF).

Grant NO. R2566B013.

Disclosure statement

The authors declare that there is no conflict of interests regarding the publication of this paper.

Funding

Kasamsuk Ungchittrakool is supported by Naresuan University (NU), and National Science, Research and Innovation Fund (NSRF). Grant NO. R2566B013.

REFERENCES

[1] Lions, P.L.; Mercier, B. Splitting Algorithms for the Sum of Two Nonlinear Operators. Siam J. Numer. Anal., 1979, 16, 964–979.

[2] Passty, G.B. Ergodic convergence to a zero of the sum of monotone operators in Hilbert space. J. Math Anal Appl., 1979, 72, 383–390.

[3] Tseng, P. A Modified Forward-Backward Splitting Method for Maximal Monotone Mappings. Siam J. Control. Optim., 2000, 38, 431–446.

[4] Alvarez, F.; Attouch, H. An inertial proximal method for maximal monotone operators via discretization of a nonlinear oscillator with damping. Set–Valued Anal., 2001, 9, 3–11.

[5] Polyak, B.T. Some methods of speeding up the convergence of iterative methods. Zh. Vychisl. Mat. Mat. Fiz., 1964, 4, 1–17.

[6] Lorenz, D.A.; Pock, T. An Inertial Forward-Backward Algorithm for Monotone Inclusions. J Math Imaging Vis., 2015, 51, 311–325.

[7] Moudafi, A.; Oliny, M. Convergence of a splitting inertial proximal method for monotone operators. J. Comput. Appl. Math., 2003, 155, 447–454.

[8] Padcharoen, A.; Kitkuan, D.; Kumam, W.; Kumam, P. Tseng methods with inertial for solving inclusion problems and application to image deblurring and image recovery problems. Comput. Math. Methods, 2021, 3, e1088.

[9] Berinde, V. Approximating fixed points of Lipschitzianpseudocontractions. Mathematics & Mathematics Education (Bethlehem, 2000), World Sci. Publishing, River Edge, 2002.

[10] Berinde, V. Iterative approximation of fixed points. Second edition. Lecture Notes in Mathematics, 1912. Springer, Berlin, 2007.

[11] Takahashi, W. Nonlinear functional analysis, Yokohama Publishers: Yokohama, 2000.

[12] Takahashi, W. Introduction to nonlinear and convex analysis, Yokohama Publishers: Yokohama, 2009.

[13] Ungchittrakool, K. Existence and convergence of fixed points for a strict pseudo-contraction via an iterative shrinking projection technique. J. Nonlinear Convex Anal., 2014, 15, 693–710.

[14] Ungchittrakool, K.; Plubtieng, S.; Artsawang, N.; Thammasiri, P. Modified Mann-type algorithm for two countable families of nonexpansive mappings and application to monotone inclusion and image restoration problems. Mathematics, 2023, 11, 2927.

[15] Artsawang, N.; Plubtieng, S.; Bagdasar, O.; Ungchittrakool, K.; Baiya, S.; Thammasiri, P. Inertial Krasnosel'skiĭ-Mann iterative algorithm with step-size parameters involving nonexpansive mappings with applications to solve image restoration problems. Carpathian J. Math., 2024, 40, 243–261.

[16] Inchan, I. split variational inclusion and fixed point problem for asymptotically nonexpansive semigroup in Hilbert spaces. Thai J. Math., 2020, 18, 1661–1675.

[17] Alvarez, F. Weak convergence of a relaxed and inertial hybrid projection-proximal point algorithm for maximal monotone operators in Hilbert space. SIAM J. Optim., 2004, 14, 773–782.

[18] Artsawang, N.; Ungchittrakool, K. Inertial Mann-type algorithm for a nonexpansive mapping to solve monotone inclusion and image restoration problems. Symmetry, 2020, 12, 750.

[19] Attouch, H.; Bolte, J.; Svaiter, B.F. Convergence of descent methods for semi-algebraic and tame problems: proximal algorithms, forward-backward splitting, and regularized Gauss-Seidel methods. Math. Program., 2009, 137 , 91–129.

[20] Baiya, S.; Plubtieng, S.; Ungchittrakool, K. An inertial shrinking projection algorithm for split equilibrium and fixed point problems in Hilbert spaces. J. Nonlinear Convex Anal., 2021, 22, 2679–2695.

[21] Baiya, S.; Ungchittrakool, K. Accelerated hybrid algorithms for nonexpansive mappings in Hilbert spaces. Nonlinear Funct. Anal. Appl., 2022, 27, 553–568.

[22] Baiya, S.; Ungchittrakool, K. Modified inertial Mann's algorithm and inertial hybrid algorithm for k-strict pseudo-contractive mappings. Carpathian J. Math., 2023, 39, 27–43.

[23] Dong, Q.L.; Yuan, H.B.; Cho, Y.J.; Rassias, Th.M. Modified inertial Mann algorithm and inertial CQ-algorithm for nonexpansive mappings. Optim. Lett., 2018, 12, 87–102.
[24] Munkong, J.; Dinh, B.V.; Ungchittrakool, K. An inertial extragradient method for solving bilevel equilibrium problems. Carpathian J. Math., 2020, 36, 91–107.
[25] Munkong, J.; Dinh, B.V.; Ungchittrakool, K. An inertial multi-step algorithm for solving equilibrium problems. J. Nonlinear Convex Anal., 2020, 21, 1981–1993.
[26] Nesterov, Y. A method for solving a convex programming problem with convergence rate $O(1/K^2)$. Dokl. Math., 1983, 27, 367–372.
[27] Gibali, A.; Thong, D.V. Tseng type methods for solving inclusion problems and its applications. Calcolo, 2018, 55.
[28] Brézis, H.; Chapitre, I.I. Operateursmaximaux monotones. North-Holland Math Stud., 1973, 5, 19–51.
[29] Bauschke, H.H.; Combettes, P.L.Convex analysis and monotone operator theory in Hilbert spaces. CMS Books in Mathematics. New York:Springer, 2011.
[30] Opial, Z. Weak convergence of the sequence of successive approximations for nonexpansive mappings. Bull. Amer. Math. Soc., 1967, 73, 591–597.
[31] Wang, Z.; Bovik, A.C.; Sheikh, H.R.; Simoncelli, E.P. Image quality assessment: from error visibility to structural similarity. IEEE Trans. Image Process., 2004, 13, 600–612.